Antiviral Research 222 (2024) 105810

Contents lists available at ScienceDirect

Antiviral Research

journal homepage: www.elsevier.com/locate/antiviral

Molecular mechanism of rhinovirus escape from the Pyrazolo[3,4-*d*] pyrimidine capsid-binding inhibitor OBR-5-340 via mutations distant from the binding pocket: Derivatives that brake resistance

Martina Richter [a], Kristin Döring [a], Dieter Blaas [b], Olga Riabova [c], Maria Khrenova [c,d], Elena Kazakova [c], Anna Egorova [c], Vadim Makarov [c,**], Michaela Schmidtke [a,*]

[a] *Jena University Hospital, Department Medical Microbiology, Section Experimental Virology, Hans-Knoell-Str. 2, 07743 Jena, Germany*
[b] *Medical University Vienna, Centre of Med. Biochem. Vienna Biocenter, Dr. Bohr Gasse 9/3, A-1030 Vienna, Austria*
[c] *Federal Research Centre "Fundamentals of Biotechnology" of the Russian Academy of Sciences (Research Centre of Biotechnology RAS), 33-2 Leninsky Prospect, 119071 Moscow, Russia*
[d] *Department of Chemistry, Lomonosov Moscow State University, 1/3 Leninskie Gory, 119991 Moscow, Russia*

ARTICLE INFO

Keywords:
Common cold
Antiviral
Pyrazolopyrimidine
Escape mutation
Molecular dynamics

ABSTRACT

Rhinoviruses (RVs) cause the common cold. Attempts at discovering small molecule inhibitors have mainly concentrated on compounds supplanting the medium chain fatty acids residing in the sixty icosahedral symmetry-related hydrophobic pockets of the viral capsid of the *Rhinovirus-A* and *-B* species. High-affinity binding to these pockets stabilizes the capsid against structural changes necessary for the release of the ss(+) RNA genome into the cytosol of the host cell. However, single-point mutations may abolish this binding. RV-B5 is one of several RVs that are naturally resistant against the well-established antiviral agent pleconaril. However, RV-B5 is strongly inhibited by the pyrazolopyrimidine OBR-5-340. Here, we report on isolation and characterization of RV-B5 mutants escaping OBR-5-340 inhibition and show that substitution of amino acid residues not only within the binding pocket but also remote from the binding pocket hamper inhibition. Molecular dynamics network analysis revealed that strong inhibition occurs when an ensemble of several sequence stretches of the capsid proteins enveloping OBR-5-340 move together with OBR-5-340. Mutations abrogating this dynamic, regardless of whether being localized within the binding pocket or distant from it result in escape from inhibition. Pyrazolo [3,4-*d*]pyrimidine derivatives overcoming OBR-5-340 escape of various RV-B5 mutants were identified. Our work contributes to the understanding of the properties of capsid-binding inhibitors necessary for potent and broad-spectrum inhibition of RVs.

1. Introduction

Rhinovirus species A, B, and *C* (80, 32, and 59 types, respectively) represent the major cause of common cold in all age groups (Esneau et al., 2022; Heikkinen and Jarvinen, 2003; Simmonds et al., 2020). *Rhinovirus A* and *C* are most prevalent and associated with more severe clinical presentations including chronic bronchiolitis, pneumonia, exacerbation of chronic obstructive pulmonary disease, and asthma (Cilloniz et al., 2022; Esneau et al., 2022; Jackson and Gern, 2022; Lee et al., 2007; Renwick et al., 2007; Royston and Tapparel, 2016; Ruuskanen et al., 2011). Rhinoviruses (RVs) circulate worldwide year-round with the peak incidence occurring in autumn and spring (Esneau et al., 2022; Moriyama et al., 2020). During the COVID-19 pandemic many countries implemented multiple complementary 'non-pharmaceutical measures', such as mask wearing, lockdown etc. to prevent SARS-CoV-2 circulation. Although this also diminished influenza virus and respiratory syncytial virus infections, it did not prevent RV circulation (Buchholz et al., 2023; Mansuy et al., 2021; Vittucci et al., 2021). This underlines the strong need for additional preventive and/or therapeutic measures to control rhinovirus-induced acute respiratory infection.

The large number of different RV types hinders the development of vaccines and small-molecule antivirals. Only a few research groups are aiming at developing molecules able to inhibit a wide spectrum of RVs ('broad-spectrum inhibitors'). The targets for these inhibitors are highly conserved regions of viral proteases, RNA polymerases, and capsid

* Corresponding author.
** Corresponding author.
E-mail addresses: makarov@inbi.ras.ru (V. Makarov), michaela.schmidtke@med.uni-jena.de (M. Schmidtke).

https://doi.org/10.1016/j.antiviral.2024.105810
Received 17 November 2023; Received in revised form 4 January 2024; Accepted 14 January 2024
Available online 18 January 2024

Nomenclature

AAS	amino acid substitutions
CPE	cytopathic effect
PI	plaque isolates
hpi	hours post infection
PCR	polymerase chain reaction
PRA	plaque reduction assay
RV-B5	rhinovirus B5
RT	reverse transcription
RVs	rhinoviruses
TCID50	tissue culture infection dose 50%
VP1-4	virus capsid proteins 1-4
WT	wild-type

proteins (Egorova et al., 2019; Patick, 2006; Rollinger and Schmidtke, 2011; Thibaut et al., 2016). Capsid-binding inhibitors of *RVs A* and *B* were considered very promising. Pleconaril, vapendavir, and the pyrazolopyrimidine OBR-5-340 represent small-molecule leads of such broad-spectrum capsid binders with proven activity *in vitro* and efficacy *in vivo* (Barnard et al., 2004; Feil et al., 2012; Groarke and Pevear, 1999; Makarov et al., 2015; Pevear et al., 1999). Nevertheless, low clinical efficacy and side effects of pleconaril and vapendavir noted in human trials prevented drug approval (Egorova et al., 2019).

All three compounds affect the early steps of the RV reproduction cycle by inhibiting its adsorption and/or uncoating through binding to a small hydrophobic pocket in the viral capsid protein 1 (VP1) (Braun et al., 2015; Feil et al., 2012; Groarke and Pevear, 1999; Makarov et al., 2015; Wald et al., 2019). A comparison of the available 3D-structures of representatives from the *Enteroviruses* genus complexed with capsid binders like pleconaril reveal quite similar binding geometry, meanwhile OBR-5-340 only partially overlaps with this binding site (Wald et al., 2019). Therefore, the spectrum of anti-RV activity of OBR-5-340 is broader and includes pleconaril-, and vapendavir-resistant RVs, for example, rhinovirus B5 (RV-B5) (Wald et al., 2019). The promising *in vitro* antiviral activity and favorable *in vivo* efficacy of OBR-5-340 together with its metabolic stability and lack of CYP induction (Makarov et al., 2015; Wald et al., 2019) indicate that this molecule could become a suitable lead compound for further optimization into an antiviral drug candidate.

In lead-to-candidate optimization, it is important to know the rate of resistance development, to identify mutations conferring resistance, and to determine structural modifications of the lead that overcome resistance. Such data are available for coxsackievirus B3 virus (Makarov et al., 2015) but not for RVs. Generally, RNA viruses exhibit high genetic variability and evolve as quasispecies (Domingo et al., 2021). Consequently, virus variants with resistance-conferring amino acid substitutions likely already exist prior to treatment with the inhibitor or emerge during treatment (Kirkegaard et al., 2016; Perales et al., 2012). Amino acid substitutions that confer low level (partial) or high-level (full) resistance to capsid-binding inhibitors of RVs were identified (Heinz et al., 1989). Such resistance-conferring amino acid substitutions were detected inside and outside of the drug-binding pocket (Braun et al., 2015; Feil et al., 2012; Groarke and Pevear, 1999; Lanko et al., 2021; Makarov et al., 2015).

To fill the gap in the knowledge of RV resistance to OBR-5-340, we aimed at (i) determining the frequency and the type (partial or full) of OBR-5-340-resistant RV-B5, (ii) identifying amino acid substitutions affecting OBR-5-340 susceptibility, (iii) explaining the underlying molecular mechanism, and (iv) evaluating the effect of resistance-conferring mutations on viral replication and thermostability. Another goal was to identify key structural features of OBR-5-340 derivatives capable of overcoming resistance.

2. Materials and methods

2.1. Compound synthesis

The phenylpyrazolo[3,4-*d*]pyrimidine-4-amines used in this study were synthesized mainly according to the scheme and synthetic procedures described in (Makarov et al., 2015). A brief description of synthetic procedure, a synthetic scheme, and compound characteristics are given in Supplementary Material 1.

2.2. Cells and viruses

HeLa Ohio cells (Flow Laboratories, USA) were grown in Eagle's minimal essential medium (MEM) supplemented with 5% calf serum (PAA, Cölbe, Germany). RV-B5 was received from the National Collection of Pathogenic Viruses, Salisbury, UK and termed RV-B5 WT1. RV-B5 WT2 was obtained by further passaging of RV-B5 WT1 for mechanism of action studies (Wald et al., 2019). RV propagation and antiviral studies were performed in MEM with 2% calf serum (test medium) in HeLa Ohio cells.

2.3. Isolation and purification of OBR-5-340-resistant RV-B5 mutants

Ten OBR-5-340-resistant plaque isolates (PI) of RV-B5 WT1 were obtained as published previously with some modifications (Braun et al., 2015; Groarke and Pevear, 1999; Makarov et al., 2015). Briefly, 10 samples of a tenfold RV-B5 WT1 dilution were incubated with 1 μM OBR-5-340 in test medium at 33 °C. After 1 h, virus suspensions were further diluted (10^{-2}, 10^{-3}, 10^{-4}) in OBR-5-340-containing (1 μM) test medium and 500 μl aliquots were transferred onto HeLa cell monolayers in 12-well culture plates. After adsorption at 33 °C for 1 h, the inoculum was removed and 1 ml test medium containing 0.4% agar ± OBR-5-340 (1 μM) was added. One mock-infected, mock-treated cell control and three mock-treated virus controls were included in all assays. After incubation at 33 °C for 4 days individual plaques were collected and two times plaque-purified in the presence of 1 μM OBR-5-340.

2.4. RNA isolation, RT-PCR, and sequencing of the capsid-protein encoding region P1

RNA was extracted by using an RNeasy Mini Kit (Qiagen, Hilden, Germany) according to the manufacturer's instructions and stored in 30 μl of RNase-free water at −80 °C. A two-step reverse transcription (RT)-polymerase chain reaction (PCR) was utilized to amplify the capsid-protein encoding P1 region of RV-B5. RT was conducted with the Omniscript RT kit (Qiagen, Hilden, Germany), the RV-B5 RT primer 5′-CTA CTT TGG GTG TCC G-3′, and 1.5 μg of RNA in a final reaction volume of 20 μl. PCR amplification was carried out using the Taq Core kit 10. Primers are listed in Supplementary Table S1 and the cycling conditions in Supplementary Table S2. Amplified DNA was purified by using the QIAquick Gel extraction kit (Qiagen, Hilden, Germany) or the QIAquick PCR purification kit (Qiagen, Hilden, Germany) and stored at −20 °C. Nucleotide sequences were determined by using fluorescence-labelled nucleotides with the GenomeLab™ DTCS Quick Start Kit (Qiagen, Hilden, Germany). RV-B5 amino acid sequences were aligned and compared to sequence **FJ445112.1** (Palmenberg et al., 2009) with BioEdit (version 5.0.9).

2.5. Amino acid sequencing by using mass spectroscopy

The amino acid sequence of the viral capsid protein VP3 of RV-B5 WT2 was confirmed by order issued to the mass spectrometry facility of the Max Perutz Labs of the Vienna Biocenter (Supplementary Material 2).

2.6. One-step virus growth analysis and thermostability studies

We focused on studying the impact of single mutations Q2131L (PI-2) and Y1201H (PI-9) on replication kinetics and thermostability studies because the interpretation of the properties of triple mutants is difficult and would remain highly speculative without reverse engineering. Semiconfluent HeLa cells grown in 4-well tissue culture plates (Nunc GmbH & Co. KG, Langenselbold), one per time point, were infected with RV-B5 WT1, PI-2 or PI-9 at a multiplicity of infection of 1 $TCID_{50}$/cell in 300 μl test medium (3 wells) or mock-infected for control (1 well) at 33 °C as described (Braun et al., 2015). At selected times infection was halted by freezing at −80 °C. After thawing, the virus titer was determined by endpoint titration. Thermostability was assessed by heating samples of RV-B5 WT1, WT2, PI-2, and PI-9 to 46 °C, 48 °C, and 50 °C. For control, samples were kept on ice for 10 min. Then, titer reduction relative to the control samples was determined.

2.7. Antiviral assays

Susceptibility of RV-B5 and resistance of all ten PI against OBR-5-340 (maximum 2.7 μM) was studied with plaque reduction assays (PRA) in confluent HeLa cells grown in 12-well plates. Three untreated virus controls and one uninfected, untreated cell control were included in all assays. Each compound concentration was tested twice. After incubation at 33 °C for 4 days, cells were fixed and stained with crystal violet, plaques were counted and used to calculate the percentage of plaque reduction as described previously (Schmidtke et al., 2001).

CPE inhibition assays were performed in one-day-old semi confluent monolayers of HeLa cells in 96 well flat-bottomed microtiter plates as published (Makarov et al., 2015; Schmidtke et al., 2001). Infection with RV-B5 WT1 and WT2 (MOI 0.01) and six selected OBR-5-340-resistant PI (MOI 0.15) resulted in nearly complete CPE at 72 h p.i.

2.8. Molecular dynamics simulations

Coordinates of heavy atoms of the RV-B5 WT complex with the OBR-5-340 were taken from the cryogenic electron microscopy (cryo-EM) structure **PDB ID: 6SK5** (Wald et al., 2019). Amino acid substitutions were manually introduced to construct a set of five OBR-5-340/RV-B5 complexes: L3221, L3221F, Y3175F, Y1201H and Q2131L (the first digit denotes the VP) as well as the triple mutant, including L1043V, E1117D, and Y3175F.

We performed simulations of 250–300 ns and analyzed only equilibrated systems that we controlled by the time dependence of the RMSD of protein heavy atoms. We checked that these curves reach plateau and performed dynamical network analysis for the different trajectory lengths: 100, 150 and 200 ns. Independently on the trajectory length, we observed the same behavior in the ligand and 1192–1195 and 1217–1219 loops region. Therefore, we suppose that this criterion is reliable and can be utilized for classification. Thus, molecular dynamics (MD) simulations were performed as follows: 50 ns system equilibration followed by the 100 ns production run for each model system. The protein macromolecule was described with CHARMM36 force field parameters (Best et al., 2012; Denning et al., 2011), OBR-5-340 with the CGenFF (Vanommeslaeghe et al., 2010) and solvent water molecules with the TIP3P (Jorgensen et al., 1983) parameters. Simulations were performed in the NPT ensemble at T = 300 K and p = 1 atm with a 1 fs integration time step. All MD simulations were carried out with the NAMD software. Dynamical network analysis (Sethi et al., 2009) was utilized by dividing the complex to communities with correlated motions within them; every amino acid was represented by a single node; the OBR-5-340 molecule was divided into three parts. Any two nodes (except the neighbors) were connected by an edge if the distance between any pair of atoms of the respective residues was less than 4 Å for more than 75% of the simulation time. Covariance and correlation matrices for dynamical network analysis were calculated with the Carma program (Glykos, 2006).

2.9. Statistical analysis

Mean and standard deviations were calculated with EXCEL2016. Linear regression was applied to derive the 50% CPE inhibitory concentration (IC_{50}) in PRA and CPE inhibition assays with EXCEL. The two-sided *t*-test was used for statistical analysis of one-step virus growth analysis with EXCEL.

3. Results

3.1. Isolation and phenotypic characterization of OBR-5-340-resistant RV-B5 variants

The highly OBR-5-340-sensitive RV-B5 (Makarov et al., 2015) was selected to evaluate resistance development. The molecular binding mechanism of OBR-5-340 to the viral capsid was deciphered by using cryo-EM structure determination of the virus/inhibitor complex (Wald et al., 2019).

The mutation frequency was determined as the fraction of virus forming plaques in the presence of a high inhibitor concentration, analogous to earlier studies (Braun et al., 2015; Groarke and Pevear, 1999; Heinz et al., 1989; Makarov et al., 2015). The frequency of RV-B5 WT1 (for the definition of WT1 and WT2 see 3.2) mutants forming plaques in the presence of OBR-5-340 was 7.5×10^{-3}.

Ten RV-B5 escape mutants were isolated from the above plaques (referred to as plaque isolates, PI 1–10, in Table 1) and phenotypically characterized. Viral escape from OBR-5-340 inhibition was confirmed in plaque reduction assays for all PI as well as in CPE inhibition assays for 6 selected PI (Fig. 1A and B). Mean dose-response curves of RV-B5 WT1 compared to PI show a strong reduction of susceptibility to OBR-5-340. The maximum compound concentration applied in plaque reduction assay of PI diminished the number of plaques by only up to 40%, indicating incomplete escape. Application of higher concentrations in CPE inhibition assays enabled the calculation of 50% inhibitory concentrations (IC_{50} values) of the PI as given in Table 1. The 41 to 557-fold-increased IC_{50} values as compared to both RV-B5 WT1 and WT2 confirmed the strongly reduced OBR-5-340 susceptibility of PI.

3.2. Amino acid substitutions detected in OBR-5-340-resistant RV-B5

Sequence analysis of the P1 region, which includes all four viral capsid proteins (VP1-4) and comparison to sequence **FJ445112.1** (Palmenberg et al., 2009) revealed a natural polymorphism at 3 positions: 1101 (asparagin, N or aspartate, D), 3004 (alanin, A or threonine, T), and 3221 (leucine, L or phenylalanine, F) marginally impacting on OBR-5-340 susceptibility against RV-B5 WT1 and WT2 (Table 1). Mass spectrometry protein sequencing essentially confirmed the covered peptides of VP3 of RV-B5 WT2 (Supplementary Material 2). Intriguingly, about 2% phenylalanine and 98% leucine was identified at position 3221, suggesting that one or the other residue might be selected by the viral propagation conditions.

One to three additional amino acid substitutions were identified in the OBR-5-340-resistant PI (Table 1). PI-1 has three substitutions: L1043V, E1117D, and Y3175F. Q2131L was detected in five PIs (PI 2–6), and, together with H3229Y, in PI-7. In addition, Q2131 was detected in PI-2 (intensity approximately 50% of the L2131 intensity). Finally, three RV-B5 plaque isolates (PI 8–10) had the substitution Y1201H. This leaves us with the single mutations Q2131L and Y1201H and/or the triple mutation L1043V, E1117D, Y3175F to be considered further. It is of note that the mutations Q2131L and Y1201H did not affect resistance against pleconaril and susceptibility to disoxaril (Table 1).

Table 1
Susceptibility of rhinovirus B5 (RV-B5) variants to pleconaril, disoxaril, and OBR-5-340.

RV-B5 wild type (WT) and plaque isolates (PI)	Amino acid substitutions compared to the sequence published by Palmenberg[a]	IC_{50} (μM)[b]			
		OBR-5-340		Pleconaril	Disoxaril
		Plaque reduction	CPE inhibition	CPE inhibition	CPE inhibition
WT1	N1101D, A3004T, L3221F	0.02 ± 0.01	0.02 ± 0.01	NA	2.66 ± 2.47
WT2	A3004T	0.10 ± 0.02	0.11 ± 0.04	NA	0.85 ± 0.50
PI-1	N1101D, **L1043V, E1117D,** A3004T, **Y3175F**	>2.7	ND	ND	ND
PI-2	N1101D, **Q2131L,** A3004T	>2.7	11.15 ± 3.15	NA	3.40 ± 1.43
PI-3	N1101D, **Q2131L,** A3004T	>2.7	ND	ND	ND
PI-4	N1101D, **Q2131L,** A3004T	>2.7	10.49 ± 1.70	NA	ND
PI-5	N1101D, **Q2131L,** A3004T	>2.7	8.52 ± 1.29	NA	ND
PI-6	N1101D, **Q2131L,** A3004T	>2.7	ND	ND	ND
PI-7	N1101D, **Q2131L,** A3004T, **H3229Y**	>2.7	ND	ND	ND
PI-8	N1101D, **Y1201H,** A3004T, L3221F	>2.7	5.09 ± 2.05	NA	ND
PI-9	N1101D, **Y1201H,** A3004T, L3221F	>2.7	4.18 ± 1.02	NA	3.55 ± 1.99
PI-10	N1101D, **Y1201H,** A3004T, L3221F	>2.7	4.90 ± 1.74	NA	ND

[a] Positions of amino acids exchanged with respect to the ones published by Palmenberg et al., (2009), are given plus 1000, 2000, or 3000 for VP1, VP2, or VP3, respectively. Amino acid substitutions detected in OBR-5-340-resistant PI but not in the two OBR-5-340-sensitive wild-type RV-B5 (WT1 and WT2) are marked in bold.

[b] The mean 50% inhibitory concentration (IC_{50}) and standard deviation determined in at least 3 independent assays; NA not active at non-cytotoxic concentrations; ND not determined.

3.3. Influence of resistance-conferring amino acid substitutions on virus replication and thermostability

Resistance-conferring amino acid substitutions might affect viral replication kinetics (Hoffmann et al., 2016; Lonberg-Holm and Noble-Harvey, 1973). The results of one-step growth kinetics of RV-B5 WT1, PI-2, and PI-9 in HeLa cells revealed a coincidence for PI-2 and PI-9. In contrast, significant differences were found between RV-B5 WT1 and PI-2, as well as RV-B5 WT1 and PI-9 from 5 to 10 h post infection (hpi) and 6–9 hpi, respectively ($p < 0.05$) (Fig. 2A). This suggests that Y1201H and Q2131L confer an advantage to viral uncoating (release of viral RNA from the capsid). Nevertheless, the maximal virus yield of RV-B5 WT1, PI-2, and PI-9 was similar at 11 and 12 hpi.

Uncoating of RVs requires conformational changes in viral capsid proteins (Fuchs and Blaas, 2010) that might be affected by amino acid substitutions. Heating RVs to ≥50 °C artificially triggers uncoating (Harutyunyan et al., 2015; Lonberg-Holm and Noble-Harvey, 1973). This results in a temperature-dependent reduction of infectious virus because, under the conditions used, the released viral RNA cannot infect (Lacroix et al., 2015; Lonberg-Holm and Noble-Harvey, 1973). As seen in Fig. 2B and in agreement with previous findings (Wald et al., 2019), RV-B5 WT2 lost 99% of its infectivity after 10 min at 48 °C, as did PI-2 and PI-9, whereas RV-B5 WT1 was somewhat more stable.

3.4. Molecular origin of different inhibitory potency of OBR-5-340 toward the RV-B5 variants

Table 1 demonstrates that amino acid substitutions in the RV-B5 escape mutants confer reduced binding potency of OBR-5-340. Two amino acid substitutions, Y1201H and Q2131L, are located close to the OBR-5-340 binding site, whereas two others in VP3 (H3229Y and Y3175F) are quite distant (Fig. 3A). The most distant one, Y3175F, affected the IC_{50} value, whereas L3221F (natural polymorphism) did not. Classical molecular dynamics simulations were performed for OBR-5-340/RV-B5 complexes: L3221, L3221F, Y3175F, Y1201H, Q2131L and for the triple mutant including L1043V, E1117D, and Y3175F to clarify these experimental observations. OBR-5-340 is located between the sequence stretches 1217-219 and 1192-195 of VP1 (Fig. 3B). Likely, formation of the complex should fix these two regions relative to each other via interactions with the inhibitor. The proper way to quantify this effect is to perform dynamical network analysis of the MD trajectory and divide the entire system into communities that are characterized by correlated motions.

For both wild-type RV-B5 amino acid sequences (Fig. 3C and D), included for control, we found that both VP1 1217–1219 and 1192–1195 fragments and OBR-5-340 belong to the same community. In case of PIs with higher IC_{50} values, the OBR-5-340 motions are correlated only with amino acid residues of VP1 1192–1195 (Fig. 3E–G). The results for the triple mutant, including L1043V, E1117D, and Y3175F correspond with that of the other PIs and are not shown. Thus, increase of the IC_{50} value can be explained by formation of more relaxed complexes in which the inhibitor does not stabilize the protein fragments that envelope it.

3.5. Identification of modified pyrazolopyrimidines with improved activity against OBR-5-340-resistant mutants

To overcome the RV-B5 resistance to OBR-5-340, we synthesized a number of N^3,6-diphenylpyrazolo [3,4-*d*]pyrimidine-4-amines containing substituents at the 3-phenyl ring (Table 2). The 3-non-substituted pyrazolo [3,4-*d*]pyrimidine RCB04166 was poorly active against the OBR-5-340-resistant mutants. The size of the halogen probably influences the antiviral activity of pyrazolo [3,4-*d*]pyrimidine: compounds with similar halogen size at the para-position of the phenyl ring (4-chloro and 4-bromo) exhibited comparable activity against OBR-5-340-resistant strains, whereas the introduction of the bulkier halogen, iodine, led to reduced activity. The smallest halogen, fluorine, resulted in a strong or even complete loss of activity of compound RCB23141-145 against OBR-5-340-resistant mutants, and the introduction of two fluorine atoms at different positions of the 3-phenyl ring did not improve the activity. However, compound RCB23137, with the slightly sterically larger methyl group compared to iodine exerted *in vitro* activity against resistant strains comparable to RCB23137 and RCB23138.

4. Discussion

In the present study, we identified amino acid substitutions in VP1 (L1043V, E1117D, Y1201H), VP2 (Q2131L), and VP3 (Y3175F) in the P1 coding region of OBR-5-340-resistant RV-B5 mutants. Based upon the

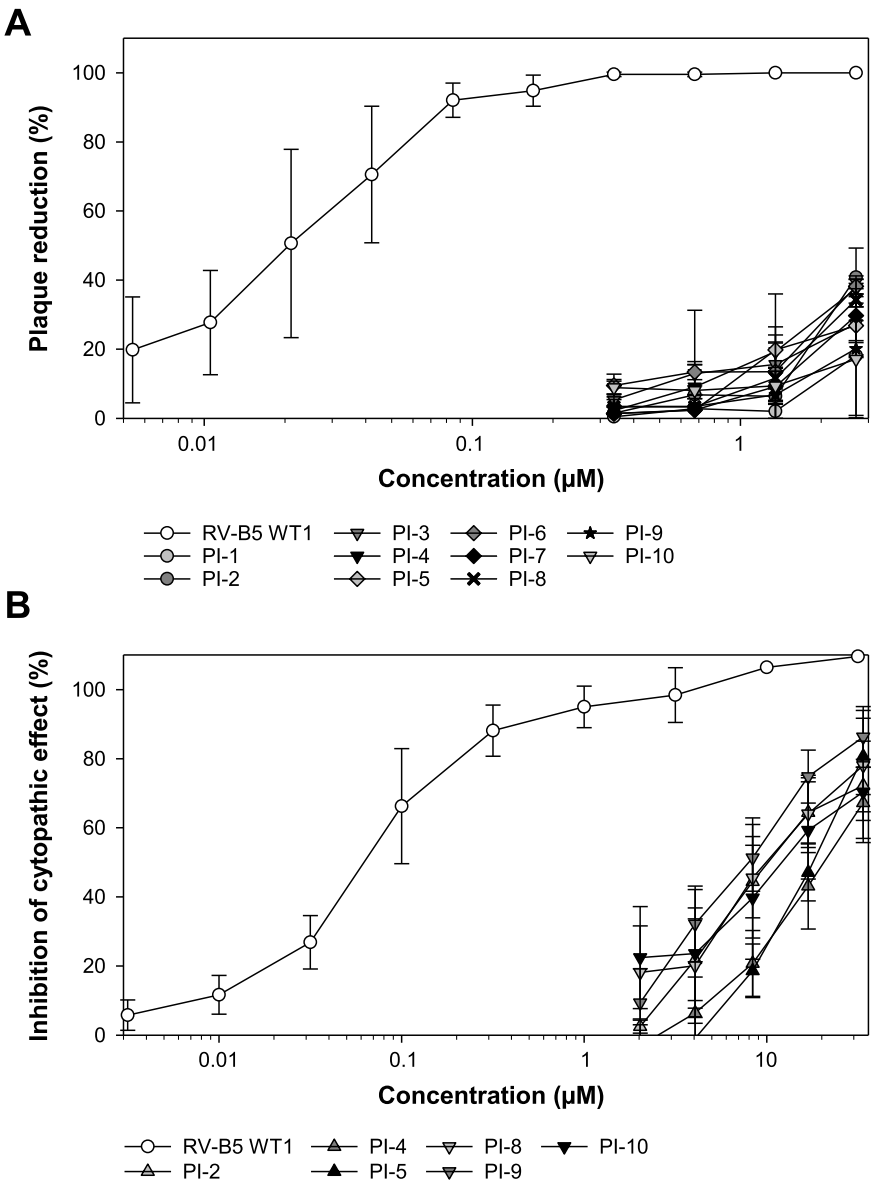

Fig. 1. Dose dependent inhibition of RV-B5 replication by OBR-5-340 in HeLa cells. (A) Plaque reduction assays were performed with RV-B5 wildtype 1 (RV-B5 WT1) and ten plaque isolates (PIs). (B) Resistance to OBR-5-340 was confirmed in CPE inhibition assays with RV-B5 WT1 and six selected PIs. Data points represent the mean and standard deviation of at least 3 assays.

cryo-EM data revealing OBR-5-340 binding to the entrance of the hydrophobic pocket in RV-B5 (Wald et al., 2019), the molecular mechanism of resistance can be explained. Y1201H and Y3175F might directly hamper OBR-5-340 binding whereas Q2131L acts indirectly by modifying the orientation of Y1201. A similar indirect mechanism of resistance is also known for the induction of oseltamivir resistance by H274Y in the neuraminidase of subtype 1 of influenza A viruses (Yadav et al., 2021; Yusuf et al., 2016).

In contrast to the amino acid substitutions conferring complete resistance of coxsackievirus B3 to OBR-5-340 (Makarov et al., 2015), those found in RV-B5 led to a partial loss of inhibitory activity. This is in good agreement with the frequency of resistant mutants in the virus population determined for OBR-5-340 that is commonly high in case of low (partial) resistance to capsid-binding inhibitors (Heinz et al., 1989). OBR-5-340-resistant PI with Y1201H and Q2131L are characterized by lower thermostability. These data suggest that the amino acid substitutions in VP1 and/or VP2 of RV-B5 WT2, PI-2, and PI-9 decreased the thermostability of the viruses. Apparently, the otherwise neutral substitution L3221F made the capsid more resistant to elevated temperature. This might be due to a cavity-filling effect of phenylalanine (Saito et al., 2000). Whether the faster increase of virus yield of OBR-5-340-resistant PI represents an advantage for human infection remains doubtful because the maximum virus yield was similar at 11 hpi.

As expected, pleconaril was inactive against both wild-type RV-B5 and the OBR-5-340-resistant mutants. This is in good agreement with the fact that naturally occurring as well as experimentally selected (cross)resistance of RVs to the majority of known capsid-binding inhibitors, including pleconaril, is mainly based on amino acid substitutions at one or two positions of VP1 in the center of the hydrophobic binding pocket (Badger et al., 1989; Feil et al., 2012; Heinz et al., 1989; Lacroix et al., 2015; Ledford et al., 2004). The capsid structures of the pleconaril-sensitive RV-B14 and RV-A16, and vapendavir-sensitive RV-A2 have been determined by X-ray crystallography to atomic resolution (Feil et al., 2012; Zhang et al., 2004). It was proposed that amino acid substitutions at position 1188 and/or 1199 in the center of the

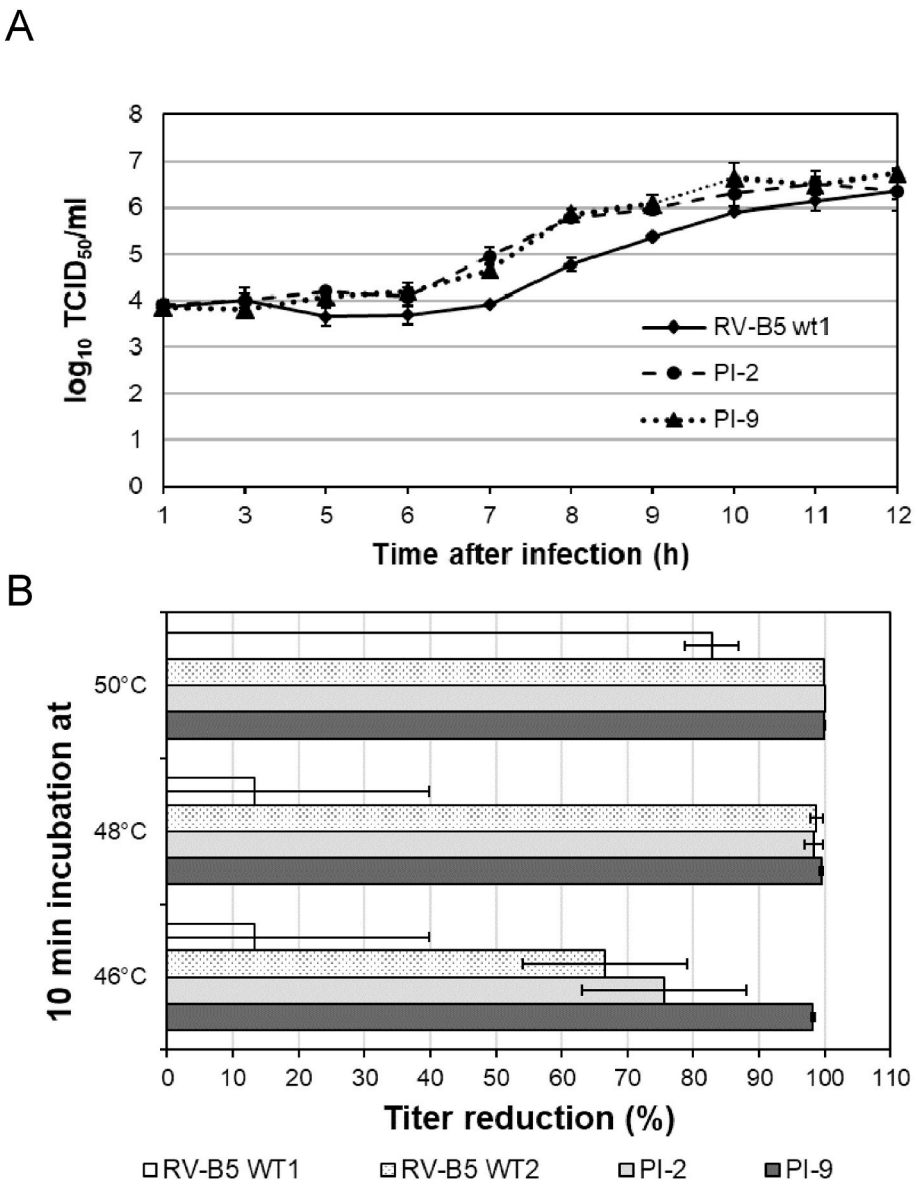

Fig. 2. Comparison of growth kinetics and thermostability of RV-B5. (A) One-step growth cycle experiments were performed with RV-B5 WT1, PI-2, and PI-9 in HeLa cells challenged with a multiplicity of infection of 1 $TCID_{50}$/cell. Virus titer was determined at the times indicated. Mean and SD of 3 parallels per time point are shown. (B) Samples of RV-B5 WT1, WT2, PI-2, and PI-9 were kept untreated or heated to 46, 48, or 50 °C for 10 min. Then, the residual infectivity in each sample was assayed and the temperature-dependent virus titer reduction was calculated. Means of 3 independent experiments with standard deviations are shown.

hydrophobic binding pocket sterically hinder inhibitor binding, in particular by interfering with its central ring (Ledford et al., 2004).

Disoxaril, an early-identified capsid-binder, inhibited wild-type RV-B5 as well as the OBR-5-340-resistant PI similarly. This was surprising because disoxaril binds also deep into the hydrophobic binding pocket like pleconaril. At the same time, in contrast to pleconaril and all other capsid-binding inhibitors with known x-ray structure of their virus complex, a second disoxaril molecule binds near to the entrance of the hydrophobic pocket in VP1, as does OBR-5-340 (Hendry et al., 1999). Our results indicate that binding of disoxaril to the entrance of the hydrophobic pocket might suffice to inhibit RV replication. In contrast to amino acid substitutions at positions 1105, 1219, and 1223 in RV-B14 (Heinz et al., 1989), the mutations Y1201H and Q2131L found in the OBR-5-340-resistant RV-B5 PI-2 and PI-9 did not reduce the antiviral activity of disoxaril.

Lower IC_{50} values for OBR-5-340 inhibition of wild-type RV-B5 are explained by more rigid structures of the corresponding complexes as seen in the correlated motions of inhibitor and the neighboring regions of VP1 in MD experiments. However, other mechanisms cannot be excluded. For example, the mutations might lead to a static change in structure that reduces the binding affinity to the drug candidate. Without determination of the 3D-structure of the mutants and the temperature factors of the amino acid residues concerned, this question will not find a definitive answer.

In the RV-B5 PIs with lower binding affinity the VP1 regions that envelope the inhibitor, move independently, conferring additional flexibility to the complex. However, small structural modifications in the 3-phenly ring of OBR-5-340 facilitated stronger inhibitor-binding to these PIs. In particular, RCB23137-139 broke the resistance.

5. Conclusions

Phenotyping and genotyping of OBR-5-340 escape mutants of RV-B5 revealed a high frequency of partial resistance type of this capsid-binding inhibitor. Amino acid substitutions near to and distinct to the binding site of OBR-5-340 were identified that directly or indirectly

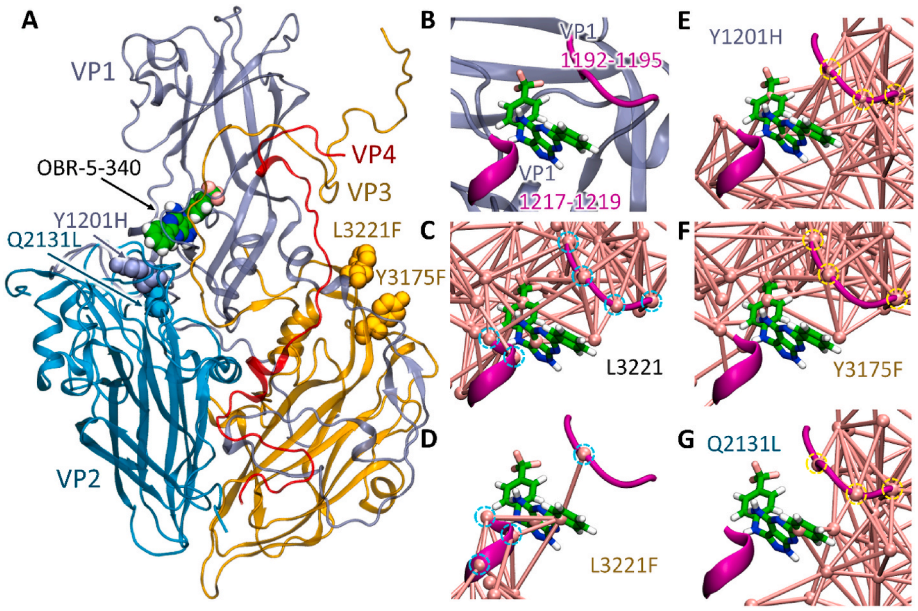

Fig. 3. (A) Complex of RV-B5 with OBR-5-340. Protein is colored by subunits: VP1 – lavender, VP2 – cyan, VP3 – yellow, VP4 – red. Amino acid residues that are substituted in the RV-B5 variants are shown as spheres and colored by subunit. OBR-5-340 is colored by atom type: C – green, N – blue, H – white and F – pink. (B) Fragments of VP1 (residues 1195–1198 and 1217–1219) that envelop OBR-5-340. (C–G) Dynamical network analysis of OBR-5-340 in the context of the RV-B5 variants. Nodes and edges of a community are shown by pink balls and sticks, respectively. For the complexes with both wild type RV-B5 variants (C) L3221 (RV-B5-WT2) and (D) L3221F (RV-B5 WT1) the residues from both VP1 regions and OBR-5-340 belong to the same community (highlighted with light blue dashed circles). In the complexes with Y1201H (E), Y3175F (F) and Q2131L (G) mutants of the RV-B5 community contain OBR-5-340 and residues from the 192–195 fragment of VP1 only (highlighted with yellow dashed circles).

Table 2
Inhibitory concentration IC_{50} (mean ± SD) of selected pyrazolo [3,4-*d*]pyrimidine-4-amines against wild-type (WT) RV-B5 and OBR-5-340-resistant PI.

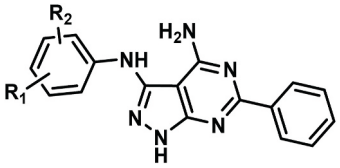

Cpd	R_1	R_2	Mean ± SD of IC_{50} (μM) against rhinovirus B5, (μM)		
			Wild-type	Y1201H	Q2131L
			WT1, WT2	PI-8 PI-9, PI-10	PI-2, PI-3, PI-4
OBR-5-340	4-CF_3	–	0.07 ± 0.06[a]	5.23 ± 1.16[a]	10.22 ± 0.97[a]
RCB04166	–	–	0.02[b]	6.86 ± 1.72	14.24 ± 5.64
RCB23137	4-Me	–	0.01 ± 0.00	0.41 ± 0.16	1.20 ± 0.49
RCB23138	4-Cl	–	0.01 ± 0.01	0.71 ± 0.10	1.66 ± 0.12
RCB23139	4-Br	–	0.01 ± 0.01	0.68 ± 0.16	1.22 ± 0.10
RCB23140	4-I	–	0.03 ± 0.01	1.00 ± 0.12	2.58 ± 0.19
RCB23141	4-F	–	0.02 ± 0.01	4.72 ± 0.70	7.21 ± 0.80
RCB23142	2-F	–	0.01 ± 0.01	1.22 ± 0.28	10.24 ± 6.14
RCB23143	3-F	4-F	0.09 ± 0.07	Not active	Not active
RCB23144	2-F	4-F	0.01 ± 0.01	2.01 ± 1.17	21.22 ± 9.90
RCB23145	3-F	5-F	0.18 ± 0.13	6.92	6.70 ± 3.91

[a] Mean of the IC_{50} values shown in Table 1 are shown here for comparison.
[b] RV-B5 WT1 (RV-B5 WT2 not tested).

hamper its inhibitory activity. According to MD simulation results changes in the dynamic features of VP1 represent one of the underlying mechanisms. For complexes with lower IC_{50} values motions of the inhibitor and neighboring protein regions are correlated. Structural modifications in the 3-phenyl ring of OBR-5-340 resulted in drug candidates with improved activity.

Grants/funding

This research did not receive any specific grant from funding agencies in the public, commercial, or not-for-profit sectors.
Patents: 50 2007 006 042.9, 50 2012 017 045.1.

CRediT authorship contribution statement

Martina Richter: Writing – review & editing, Validation, Methodology, Investigation, Formal analysis. **Kristin Döring:** Writing – review & editing, Investigation, Formal analysis, Data curation. **Dieter Blaas:** Writing – original draft, Visualization, Validation, Formal analysis, Data curation. **Olga Riabova:** Investigation, Formal analysis, Data curation. **Maria Khrenova:** Writing – original draft, Validation, Investigation, Formal analysis, Data curation. **Elena Kazakova:** Writing – review & editing, Investigation, Formal analysis, Data curation. **Anna Egorova:** Writing – original draft, Investigation, Formal analysis, Data curation. **Vadim Makarov:** Writing – original draft, Validation, Supervision, Data curation, Conceptualization. **Michaela Schmidtke:** Writing – original draft, Validation, Supervision, Formal analysis, Data curation, Conceptualization.

Declaration of competing interest

The authors declare that they have no known competing financial interests or personal relationships that could have appeared to influence the work reported in this paper.

Data availability

Data will be made available on request.

Acknowledgements

We thank Birgit Jahn and Christin Walther for technical support.

Appendix A. Supplementary data

Supplementary data to this article can be found online at https://doi.org/10.1016/j.antiviral.2024.105810.

References

Badger, J., Krishnaswamy, S., Kremer, M.J., Oliveira, M.A., Rossmann, M.G., Heinz, B.A., Rueckert, R.R., Dutko, F.J., McKinlay, M.A., 1989. Three-dimensional structures of drug-resistant mutants of human rhinovirus 14. J. Mol. Biol. 207, 163–174.

Barnard, D.L., Hubbard, V.D., Smee, D.F., Sidwell, R.W., Watson, K.G., Tucker, S.P., Reece, P.A., 2004. In vitro activity of expanded-spectrum pyridazinyl oxime ethers related to pirodavir: novel capsid-binding inhibitors with potent antipicornavirus activity. Antimicrob. Agents Chemother. 48, 1766–1772.

Best, R.B., Zhu, X., Shim, J., Lopes, P.E., Mittal, J., Feig, M., Mackerell Jr., A.D., 2012. Optimization of the additive CHARMM all-atom protein force field targeting improved sampling of the backbone phi, psi and side-chain chi(1) and chi(2) dihedral angles. J. Chem. Theor. Comput. 8, 3257–3273.

Braun, H., Kirchmair, J., Williamson, M.J., Makarov, V.A., Riabova, O.B., Glen, R.C., Sauerbrei, A., Schmidtke, M., 2015. Molecular mechanism of a specific capsid binder resistance caused by mutations outside the binding pocket. Antivir. Res. 123, 138–145.

Buchholz, U., Lehfeld, A.S., Tolksdorf, K., Cai, W., Reiche, J., Biere, B., Durrwald, R., Buda, S., 2023. Respiratory infections in children and adolescents in Germany during the COVID-19 pandemic. J. Health Monit. 8, 20–38.

Cilloniz, C., Luna, C.M., Hurtado, J.C., Marcos, M.A., Torres, A., 2022. Respiratory viruses: their importance and lessons learned from COVID-19. Eur. Respir. Rev. 31.

Denning, E.J., Priyakumar, U.D., Nilsson, L., Mackerell Jr., A.D., 2011. Impact of 2'-hydroxyl sampling on the conformational properties of RNA: update of the CHARMM all-atom additive force field for RNA. J. Comput. Chem. 32, 1929–1943.

Domingo, E., Garcia-Crespo, C., Lobo-Vega, R., Perales, C., 2021. Mutation rates, mutation frequencies, and proofreading-repair activities in RNA virus genetics. Viruses 13.

Egorova, A., Ekins, S., Schmidtke, M., Makarov, V., 2019. Back to the future: advances in development of broad-spectrum capsid-binding inhibitors of enteroviruses. Eur. J. Med. Chem. 178, 606–622.

Esneau, C., Duff, A.C., Bartlett, N.W., 2022. Understanding rhinovirus circulation and impact on illness. Viruses 14.

Feil, S.C., Hamilton, S., Krippner, G.Y., Lin, B., Luttick, A., McConnell, D.B., Nearn, R., Parker, M.W., Ryan, J., Stanislawski, P.C., Tucker, S.P., Watson, K.G., Morton, C.J., 2012. An orally available 3-ethoxybenzisoxazole capsid binder with clinical activity against human rhinovirus. ACS Med. Chem. Lett. 3, 303–307.

Fuchs, R., Blaas, D., 2010. Uncoating of human rhinoviruses. Rev. Med. Virol. 20, 281–297.

Glykos, N.M., 2006. Software news and updates. Carma: a molecular dynamics analysis program. J. Comput. Chem. 27, 1765–1768.

Groarke, J.M., Pevear, D.C., 1999. Attenuated virulence of pleconaril-resistant coxsackievirus B3 variants. J. Infect. Dis. 179, 1538–1541.

Harutyunyan, S., Sedivy, A., Kohler, G., Kowalski, H., Blaas, D., 2015. Application of FCS in studies of rhinovirus receptor binding and uncoating. Methods Mol. Biol. 1221, 83–100.

Heikkinen, T., Jarvinen, A., 2003. The common cold. Lancet 361, 51–59.

Heinz, B.A., Rueckert, R.R., Shepard, D.A., Dutko, F.J., McKinlay, M.A., Fancher, M., Rossmann, M.G., Badger, J., Smith, T.J., 1989. Genetic and molecular analyses of spontaneous mutants of human rhinovirus 14 that are resistant to an antiviral compound. J. Virol. 63, 2476–2485.

Hendry, E., Hatanaka, H., Fry, E., Smyth, M., Tate, J., Stanway, G., Santti, J., Maaronen, M., Hyypia, T., Stuart, D., 1999. The crystal structure of coxsackievirus A9: new insights into the uncoating mechanisms of enteroviruses. Structure 7, 1527–1538.

Hoffmann, A., Schade, D., Kirchmair, J., Clement, B., Sauerbrei, A., Schmidtke, M., 2016. Platform for determining the inhibition profile of neuraminidase inhibitors in an influenza virus N1 background. J. Virol. Methods 237, 192–199.

Jackson, D.J., Gern, J.E., 2022. Rhinovirus infections and their roles in asthma: etiology and exacerbations. J. Allergy Clin. Immunol. Pract. 10, 673–681.

Jorgensen, W.L., Chandrasekhar, J., Madura, J.D., Impey, R., Klein, M.L., 1983. Comparison of simple potential functions for simulating liquid water description. J. Chem. Phys. 79, 926–935.

Kirkegaard, K., van Buuren, N.J., Mateo, R., 2016. My Cousin, My Enemy: quasispecies suppression of drug resistance. Curr. Opin. Virol. 20, 106–111.

Lacroix, C., Laconi, S., Angius, F., Coluccia, A., Silvestri, R., Pompei, R., Neyts, J., Leyssen, P., 2015. In vitro characterisation of a pleconaril/pirodavir-like compound with potent activity against rhinoviruses. Virol. J. 12, 106.

Lanko, K., Sun, L., Froeyen, M., Leyssen, P., Delang, L., Mirabelli, C., Neyts, J., 2021. Comparative analysis of the molecular mechanism of resistance to vapendavir across a panel of picornavirus species. Antivir. Res. 195, 105177.

Ledford, R.M., Patel, N.R., Demenczuk, T.M., Watanyar, A., Herbertz, T., Collett, M.S., Pevear, D.C., 2004. VP1 sequencing of all human rhinovirus serotypes: insights into genus phylogeny and susceptibility to antiviral capsid-binding compounds. J. Virol. 78, 3663–3674.

Lee, W.M., Kiesner, C., Pappas, T., Lee, I., Grindle, K., Jartti, T., Jakiela, B., Lemanske Jr., R.F., Shult, P.A., Gern, J.E., 2007. A diverse group of previously unrecognized human rhinoviruses are common causes of respiratory illnesses in infants. PLoS One 2, e966.

Lonberg-Holm, K., Noble-Harvey, J., 1973. Comparison of in vitro and cell-mediated alteration of a human Rhinovirus and its inhibition by sodium dodecyl sulfate. J. Virol. 12, 819–826.

Makarov, V.A., Braun, H., Richter, M., Riabova, O.B., Kirchmair, J., Kazakova, E.S., Seidel, N., Wutzler, P., Schmidtke, M., 2015. Pyrazolopyrimidines: potent inhibitors targeting the capsid of rhino- and enteroviruses. ChemMedChem 10, 1629–1634.

Mansuy, J.M., Bourcier, M., Tremeaux, P., Dimeglio, C., Izopet, J., 2021. COVID-19 pandemic period, where are the seasonal viruses? J. Med. Virol. 93, 4097–4098.

Moriyama, M., Hugentobler, W.J., Iwasaki, A., 2020. Seasonality of respiratory viral infections. Annu. Rev. Virol. 7, 83–101.

Palmenberg, A.C., Spiro, D., Kuzmickas, R., Wang, S., Djikeng, A., Rathe, J.A., Fraser-Liggett, C.M., Liggett, S.B., 2009. Sequencing and analyses of all known human rhinovirus genomes reveal structure and evolution. Science 324, 55–59.

Patick, A.K., 2006. Rhinovirus chemotherapy. Antivir. Res. 71, 391–396.

Perales, C., Iranzo, J., Manrubia, S.C., Domingo, E., 2012. The impact of quasispecies dynamics on the use of therapeutics. Trends Microbiol. 20, 595–603.

Pevear, D.C., Tull, T.M., Seipel, M.E., Groarke, J.M., 1999. Activity of pleconaril against enteroviruses. Antimicrob. Agents Chemother. 43, 2109–2115.

Renwick, N., Schweiger, B., Kapoor, V., Liu, Z., Villari, J., Bullmann, R., Miething, R., Briese, T., Lipkin, W.I., 2007. A recently identified rhinovirus genotype is associated with severe respiratory-tract infection in children in Germany. J. Infect. Dis. 196, 1754–1760.

Rollinger, J.M., Schmidtke, M., 2011. The human rhinovirus: human-pathological impact, mechanisms of antirhinoviral agents, and strategies for their discovery. Med. Res. Rev. 31, 42–92.

Royston, L., Tapparel, C., 2016. Rhinoviruses and respiratory enteroviruses: not as simple as ABC. Viruses 8.

Ruuskanen, O., Lahti, E., Jennings, L.C., Murdoch, D.R., 2011. Viral pneumonia. Lancet 377, 1264–1275.

Saito, M., Kono, H., Morii, H., Uedaira, H., Tahirov, T.H., Ogata, K., Sarai, A., 2000. Cavity-filling mutations enhance protein stability by lowering the free energy of native state. J. Phys. Chem. B 104, 3705–3711.

Schmidtke, M., Schnittler, U., Jahn, B., Dahse, H., Stelzner, A., 2001. A rapid assay for evaluation of antiviral activity against coxsackie virus B3, influenza virus A, and herpes simplex virus type 1. J. Virol. Methods 95, 133–143.

Sethi, A., Eargle, J., Black, A.A., Luthey-Schulten, Z., 2009. Dynamical networks in tRNA: protein complexes. Proc. Natl. Acad. Sci. U. S. A. 106, 6620–6625.

Simmonds, P., Gorbalenya, A.E., Harvala, H., Hovi, T., Knowles, N.J., Lindberg, A.M., Oberste, M.S., Palmenberg, A.C., Reuter, G., Skern, T., Tapparel, C., Wolthers, K.C., Woo, P.C.Y., Zell, R., 2020. Recommendations for the nomenclature of enteroviruses and rhinoviruses. Arch. Virol. 165, 793–797.

Thibaut, H.J., Lacroix, C., De Palma, A.M., Franco, D., Decramer, M., Neyts, J., 2016. Toward antiviral therapy/prophylaxis for rhinovirus-induced exacerbations of chronic obstructive pulmonary disease: challenges, opportunities, and strategies. Rev. Med. Virol. 26, 21–33.

Vanommeslaeghe, K., Hatcher, E., Acharya, C., Kundu, S., Zhong, S., Shim, J., Darian, E., Guvench, O., Lopes, P., Vorobyov, I., Mackerell Jr., A.D., 2010. CHARMM general force field: a force field for drug-like molecules compatible with the CHARMM all-atom additive biological force fields. J. Comput. Chem. 31, 671–690.

Vittucci, A.C., Piccioni, L., Coltella, L., Ciarlitto, C., Antilici, L., Bozzola, E., Midulla, F., Palma, P., Perno, C.F., Villani, A., 2021. The disappearance of respiratory viruses in children during the COVID-19 pandemic. Int. J. Environ. Res. Publ. Health 18.

Wald, J., Pasin, M., Richter, M., Walther, C., Mathai, N., Kirchmair, J., Makarov, V.A., Goessweiner-Mohr, N., Marlovits, T.C., Zanella, I., Real-Hohn, A., Verdaguer, N., Blaas, D., Schmidtke, M., 2019. Cryo-EM structure of pleconaril-resistant rhinovirus-B5 complexed to the antiviral OBR-5-340 reveals unexpected binding site. Proc. Natl. Acad. Sci. U. S. A. 116, 19109–19115.

Yadav, M., Igarashi, M., Yamamoto, N., 2021. Dynamic residue interaction network analysis of the oseltamivir binding site of N1 neuraminidase and its H274Y mutation site conferring drug resistance in influenza A virus. PeerJ 9, e11552.

Yusuf, M., Mohamed, N., Mohamad, S., Janezic, D., Damodaran, K.V., Wahab, H.A., 2016. H274Y's effect on oseltamivir resistance: what happens before the drug enters the binding site. J. Chem. Inf. Model. 56, 82–100.

Zhang, Y., Simpson, A.A., Ledford, R.M., Bator, C.M., Chakravarty, S., Skochko, G.A., Demenczuk, T.M., Watanyar, A., Pevear, D.C., Rossmann, M.G., 2004. Structural and virological studies of the stages of virus replication that are affected by antirhinovirus compounds. J. Virol. 78, 11061–11069.